Differences between Cardiac and Skeletal Troponin Interaction with the Thin Filament Probed by Troponin Exchange in Skeletal Myofibrils

Zhenyun Yang,[†] Marie Yamazaki,[‡] Qingwu W. Shen,[‡] and Darl R. Swartz[‡*]
[†]Herman B. Wells Center for Pediatric Research, Department of Pediatrics, Indiana University School of Medicine, Indianapolis, Indiana 46202; and [‡]Department of Animal Sciences, College of Agriculture, Purdue University, West Lafayette, Indiana 47907

ABSTRACT Troponin (Tn) is the calcium-sensing protein of the thin filament. Although cardiac troponin (cTn) and skeletal troponin (sTn) accomplish the same function, their subunit interactions within Tn and with actin-tropomyosin are different. To further characterize these differences, myofibril ATPase activity as a function of pCa and labeled Tn exchange in rigor myofibrils was used to estimate Tn dissociation rates from the nonoverlap and overlap region as a function of pCa. Measurement of ATPase activity showed that skeletal myofibrils containing >96% cTn had a higher pCa 9 ATPase activity than, but similar pCa 4 activity to, sTn-containing myofibrils. Analysis of the pCa–ATPase activity relation showed that cTn myofibrils were more calcium sensitive but less cooperative ($pCa_{50} = 6.14$, $n_H = 1.46$) than sTn myofibrils ($pCa_{50} = 5.90$, $n_H = 3.36$). The time course of labeled Tn exchange at pCa 9 and 4 were quite different between cTn and sTn. The apparent cTn dissociation rates were ~2–10-fold faster than sTn under all the conditions studied. The apparent dissociation rates for cTn were 5×10^{-3} min^{-1}, 150×10^{-3} min^{-1}, and 260×10^{-3} min^{-1}, whereas for sTn they were 0.6×10^{-3} min^{-1}, 88×10^{-3} min^{-1}, and 68×10^{-3} min^{-1} for the nonoverlap region at pCa 9, nonoverlap region at pCa 4, and overlap region at pCa 4, respectively. Normalization of the apparent dissociation rates gives 1:30:50 for cTn compared with 1:150:110 for sTn (nonoverlap at pCa 9:nonoverlap at pCa 4:overlap at pCa 4) suggesting that calcium has a smaller influence, whereas strong cross-bridges have a larger influence on cTn dissociation compared with sTn. The higher cTn dissociation rate in the nonoverlap region and ATPase activity at pCa 9 suggest that it gives a less off or inactive thin filament. Analysis of the intensity ratio (after a short time of exchange) as a function of pCa showed that cTn had greater calcium sensitivity but lower cooperativity than sTn. In addition, the magnitude of the change in intensity ratio going from pCa 9 to 4 was less for cTn than sTn. These data suggest that the influence of calcium on cTn exchange is less than sTn even though calcium can activate ATPase activity to a similar extent in cTn compared with sTn myofibrils. This may be explained partially by cTn being less off or inactive at pCa 9. Modeling of the intensity profiles obtained after Tn exchange at pCa 5.8 suggest that the profiles are best explained by a model that includes a long-range cross-bridge effect that grades with distance from the rigor cross-bridge for both cTn and sTn.

INTRODUCTION

Troponin (Tn) is the protein switch in striated muscle that transduces an increase in cytosolic calcium into force production by controlling the position of tropomyosin (Tm) on the thin filament to regulate the interaction of myosin with actin (1). It is a heterotrimeric protein made of TnT, the Tm binding subunit, TnI, the inhibitory and/or actin-Tm binding subunit, and TnC, the calcium binding subunit (2). The general mechanism involved in controlling muscle contraction is similar between cardiac and skeletal Tn isoforms, but the specific molecular interactions between the subunits and between the subunits and actin-Tm are different (3–5). At the organ level, skeletal muscle can increase force production by recruiting more cells to contract, whereas cardiac muscle cannot. To increase force production, contraction at the cardiac cell level is modulated by the calcium transient (6), sarcomere length (7,8), and phosphorylation of thin (5) and thick (9) filament proteins. These latter two mechanisms either directly or indirectly involve Tn.

Comparison of fast skeletal (s) and cardiac (c) muscle contraction as a function of calcium showed that skeletal muscle is slightly more calcium sensitive and has higher cooperativity of calcium activation (10). Differences in the Tn isoforms may explain some of the differences in calcium activation. The largest functional difference is in TnC, where cTnC binds only one calcium ion in the regulatory domain (11) compared with two in sTnC (12). In addition, cTnC's apparent conformational change on calcium binding is much smaller and it binds the regulatory domain of TnI with a lower affinity (13). Physiological studies showed that substitution of cTnC for sTnC in skeletal fibers resulted in lower cooperativity, calcium sensitivity, and maximal force (14,15). Piroddi et al. (16) found that exchange of cTn for sTn in myofibrils resulted in lower cooperativity but higher calcium sensitivity and the same maximal force level. They concluded that the mismatch in Tn subunit isoforms was primarily responsible for depressing calcium activation in the TnC substitution experiments; however, the increase in calcium sensitivity in cTn skeletal myofibrils was difficult to reconcile with the functional features of cTnC. They proposed that the calcium sensitizing effect of cTn resulted from the thin filament not being as inactive. This concept was also proposed by Maytum et al. (17), who showed that cTn thin filaments were less in the off state or inactive than sTn thin filaments. Another difference in cTn myofibrils compared with sTn myofibrils is the apparent feedback of

Submitted September 8, 2008, and accepted for publication April 14, 2009.

*Correspondence: drswartz@purdue.edu

Editor: Malcolm Irving.

0006-3495/09/07/0183/12 $2.00

doi: 10.1016/j.bpj.2009.04.023

strong cross-bridges on calcium binding by TnC (18–20). Strong cross-bridges enhance calcium binding by Tn more in cardiac than in skeletal myofibrils. The molecular mechanisms responsible for this are poorly understood (21) but may involve the less-favored cTnC-cTnI regulatory interaction (13).

Recent studies on thin filament regulation propose a three-state model for the reconstituted thin filament (22,23) that includes the B (blocked or off) state, C (closed) state, and M (on) state. The equilibrium between the states is shifted from mostly the B to the C state by calcium and from the B or C state to the M state by strong cross-bridges (24,25). Tn and Tm are involved in the calcium sensitivity and cooperativity of the equilibrium between the states but the molecular mechanisms are not well understood (25–27). This model has been tested in the intact filament lattice of the isolated myofibril using fluorescent S1 binding and the data strongly support the model (28–30). In rigor or Mg-ADP, the strong cross-bridges in the overlap region result in the thin filament being in the M state independent of calcium (Fig. 1). The non-overlap region of the thin filament can be in any of the three states depending on the calcium and fluorescent S1 concentration. The rate of labeled Tn exchange was recently used to study thin filament regulation in isolated myofibrils (31). The rate of exchange is limited by the dissociation rate of the thin filament bound Tn and thus is a measure of Tn dissociation rate. The hypothesis for these experiments is that strong Tn interactions with the thin filament result in a slow exchange rate, whereas weaker interactions result in a faster exchange rate. The faster exchange rate results from the regulatory domain of TnI switching from actin-Tm to the regulatory domain of TnC (Fig. 1). The exchange rate was dependent on calcium concentration and strong cross-bridges. It was the slowest in the nonoverlap region at low calcium but ~200-fold faster in this same region with high calcium. The overlap region exchange rate was 100-fold faster than the non-overlap region at low calcium because there were strong cross-bridges in this region. The influence of calcium on the nonoverlap region exchange rate was further studied using TnC mutants or graded calcium levels. The data suggest that the calcium-induced, large increase in Tn exchange rate was mediated by switching of the regulatory domain of TnI from actin-Tm to the regulatory domain of TnC, supporting the hypothesis. These myofibril studies also demonstrated a long-range influence of the strong cross-bridge in the non-overlap region of the thin filament proximal to the overlap region. This was explained by cooperative effects of the strong cross-bridge on the thin filament, likely mediated by Tm. Other structural studies (32) and several biochemical studies have suggested a similar mechanism (25,33,34).

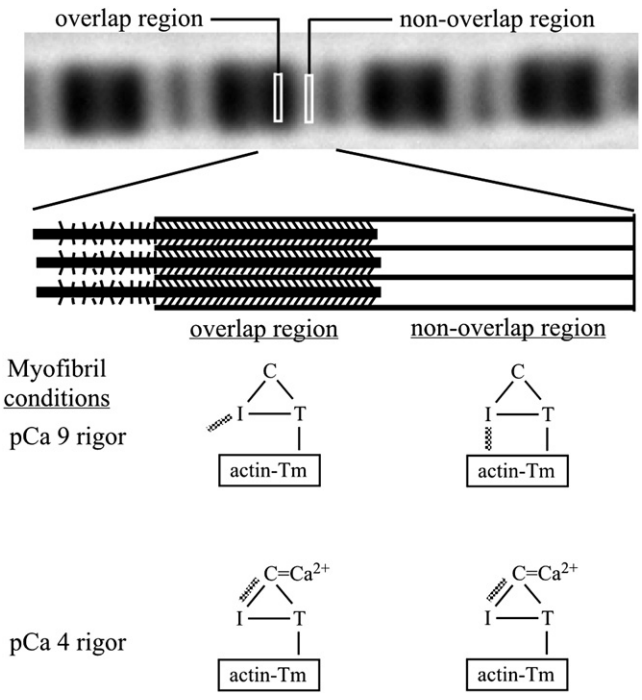

FIGURE 1 Schematic of the different regions of the thin filament at pCa 9 and 4. Upper image is a phase-contrast image of a myofibril with a schematic of the half sarcomere below. The thin filament of the half sarcomere is divided into the overlap and nonoverlap regions. The nonoverlap region under rigor condition at pCa 9 is mostly B state, whereas it is mostly C state at pCa 4. The overlap region is M state for both pCa 9 and 4 because of the presence of strong cross-bridges. The troponin subunit interactions with actin-Tm in the different regions at pCa 9 and 4 are shown with the regulatory domain of TnI having a hatched line.

In the experiments described below, myofibrillar ATPase assays and the kinetics of labeled Tn exchange in myofibrils were used to characterize the differences between sTn and cTn interaction with the thin filament. The primary goal was to determine if the influence of calcium on the B-state-to-C-state equilibrium is different between sTn and cTn. Cardiac Tn was exhaustively exchanged into skeletal myofibrils and these myofibrils were compared with sTn-exchanged myofibrils. These studies address the differences in Tn isoforms per se and not differences between cardiac and skeletal thin filaments. The experiments showed that although cTn could fully activate myofibrillar ATPase activity, the calcium sensitivity, cooperativity, and Tn exchange rate were quite different. These data can be partially explained by differences in the B-state-to-C-state equilibrium between cTn and sTn.

METHODS

Protein isolation

Rabbit white muscle was used as the source for skeletal myofibrils and sTn. Bovine cardiac muscle was used as the source for cTn. Skeletal Tn, sTnT, and cTn were isolated as described in Potter (35), with minor modifications. Myofibrils were isolated from rabbit psoas as described in Swartz et al. (28). Cardiac Tn and sTn were labeled with Alexa 488 maleimide (Invitrogen, Carlsbad, CA) as described in Swartz et al. (31), with the label being mostly in TnI for sTn and TnT for cTn.

Solutions

Buffers for Tn exchange experiments were made to specified free calcium levels (pCa 9 to 4) and contained 20 mM PIPES (pH 7.0), 4 mM EGTA,

4 mM (free) Mg^{2+}, 1 mM NaN_3, 1 mM DTT, 1 mg/mL BSA (unless noted otherwise), total calcium to get the specified free calcium, and 200 mM ionic strength via KCl. Buffers for ATPase assays contained 1 mM MgATP with total Mg^{2+}, calcium, and KCl adjusted to give the same free Mg^{2+} and calcium levels and ionic strength as for the exchange experiments. The program of Fabiato (36) was used to formulate the buffers.

Exchange of cTn for sTn

Myofibrils in pCa 4 buffer were incubated at 25°C three times for 2 h each using 0.25 mg/mL Tn and 0.5 mg/mL myofibrils. The myofibrils were collected by centrifugation at 1000 × *g* for 10 min, and the supernatant removed and replaced with an equal volume of pCa 4 buffer containing 0.25 mg/mL Tn. After the third exchange, the myofibrils were collected by centrifugation, washed twice with 0.33 volumes (relative to the initial volume) of pCa 9 buffer, and resuspended in a minimal volume of pCa 9 buffer, and the myofibril protein concentration was measured. Myofibrils were stored on wet ice and used within 4 days. For pCa 9 and 4 ATPase assays, exchange was done with labeled cTn (designated A488 cTn), unlabeled cTn (designated cTn myofibrils for Figs. 4–8), and a control of unlabeled sTn (designated sTn myofibrils for Figs. 4–8). For pCa–ATPase assays and labeled Tn exchange, cTn and sTn myofibrils were used but the myofibrils and Tns were from different preparations. The same protocol for Tn exchange was used for all experiments. These preparations gave slightly different pCa 4 results (see Fig. 4 compared with Fig. 5). The extent of cTn exchange for sTn was characterized by immunoblotting for sTnT. Samples were prepared and loaded onto 12% SDS-PAGE gels as described in Fritz et al. (37) using 4 μg of myofibril protein per lane and known sTnT amounts (extinction coefficient = 0.504 mL/mg at 280 nm). After protein transfer, the membrane was blocked with nonfat dry milk and then incubated with a 1:4000 dilution of a monoclonal anti-sTnT antibody (clone JLT-12; Sigma, St. Louis, MO), followed by a 1:10,000 dilution of goat antimouse IgG-horse radish peroxidase (Jackson Immunolabs, West Grove, PA). Color was developed by incubation with 0.5 mg/mL 3,3′- diaminobenzidine, 0.5 mg/mL nickel chloride, and 0.015% H_2O_2 in 0.1 M Tris (pH 7.6). After color development, the membrane was washed, air dried, and scanned on a flatbed scanner in 8-bit grayscale. The digital image was inverted and the bands were analyzed by segmentation analysis as described in Swartz (38).

Assays

Labeled protein concentration was determined using the BCA assay with unlabeled proteins as standards and extinction coefficients (at 280 nm) of 0.45 mL/mg for sTn and cTn. The molecular weight of the proteins used to calculate concentrations were 70,000 and 75,000 g/mol for sTn and cTn, respectively. Labeling ratios were 0.9–1.1 mol dye/mol protein for both proteins. Myofibril protein concentration was determined by the Biuret assay with BSA as the standard. ATPase assays were done at room temperature as described in Swartz et al. (39) in a final volume of 100 μL at 0.1 mg/mL myofibril protein using the buffers described above. The data were fitted to a sigmoid logistic equation to obtain the pCa_{50} and n_H with GraphPad Prism software (GraphPad Software, La Jolla, CA).

Labeled Tn exchange reaction

The apparent rate of Tn dissociation was measured using the labeled Tn exchange as described in Swartz et al. (31) with modifications. Labeled cTn was exchanged into cTn myofibrils, whereas labeled sTn was exchanged into sTn myofibrils. The reaction was stopped by centrifugation at 13,000 × *g* for 15 s followed by washing one time with pCa 9 buffer at 0.1 mg/mL BSA, then mounting and fixing. Slides were stored at −20°C until imaging.

Imaging and image analysis

Myofibrils were imaged using methods modified from Swartz et al. (31). Microscopy was done using a Leica DMC6000B microscope (Leica Microsystems, Wetzlar, Germany) equipped with a 100× oil-immersion phase-contrast lens. Image collection was via a CoolSnap HQ camera (Roper Scientific, Tucson, AZ) attached to the bottom port of the microscope. A computer equipped with IPLab v. 3.9 Mac software (Bio-Vision Technologies, Exton, PA) controlled the microscope filters, shutters, light path, and camera. Myofibrils were selected by scanning across the field and finding myofibrils that: 1), had the desired sarcomere length; 2), were a single myofibril; and 3), had three or more contiguous sarcomeres in the same plane of focus. A script was used to collect the phase-contrast image. If the myofibril was in good focus, the operator activated the script to collect the Alexa 488 (Tn) image and saved the images to disk. Camera exposure was with auto-exposure to 2000 maximum intensity units (below camera saturation). The ratio of the intensity in the nonoverlap region to that of the overlap region was measured by centering the region of interest (66 nm wide × 443 nm tall with respect to the long axis of the sarcomere) for the overlap region at 900 nm and the nonoverlap region at 300 nm from the *Z*-line. Initial *Z*-line position was determined from the phase-contrast image. Because of subtle frame shifts between the images, final *Z*-line position was determined from the Tn image. These region-of-interest locations were based on modeling of an intensity profile as the sum of Gaussian intensities (see the Supporting Material) from the Tn sites along the thin filament for sarcomeres at lengths of 2.75–2.85 μm.

Intensity ratio analysis and image presentation

The apparent Tn dissociation rates at pCa 4 were determined by nonlinear regression to the equation nonoverlap/overlap intensity = $[(1 - \exp(-k_{no}*t))/(1 - \exp(-k_{ol}*t))] + C$ where k_{no} and k_{ol} are the apparent rates (min^{-1}) of Tn dissociation from the nonoverlap and overlap regions respectively, t is time in minutes, and C is the offset. Modeling of the equation shows that at near time zero, the intensity ratio is the ratio of the dissociation rates, whereas the midpoint of the change in intensity ratio gives the magnitude of the rates. Theoretically, C should equal zero at infinite time. Practically, there was additional labeled Tn incorporated near the *Z*-line for both cTn and sTn at pCa 4 such that it was not zero and this was observed previously (31). Fitting is most robust when the ratio of the rates is ~0.3–10. For pCa 9, where ratio is small, the data were fitted to a single exponential after baseline correction. Myofibrils included in the analysis had a sarcomere length range of 2.7–2.9 μm. Myofibrils with the sarcomere length nearest 2.8 μm and nearest the mean intensity ratio for each incubation time and/or pCa were used for presentation and processed as described in (31). The intensity ratio as a function of pCa after 8 min of exchange was fitted to a sigmoid logistic equation to estimate the pCa_{50} and n_H for the change in ratio.

Intensity profiles and intensity profile modeling

Intensity profiles were obtained from the 8-bit images as described in Swartz et al. (31). To extract more information from the intensity profile, modeling of the profile as the sum of individual Gaussian profiles along the length of the sarcomere was done. This approach is similar to that done by Littlefield and Fowler (40). See the Supporting Material for details.

RESULTS

Extent and location of exchange and functionality of labeled cTn

It is essential to have extensive (>90%) exchange of cTn for sTn in the skeletal myofibrils and that the exchange be uniform along the thin filament for the current studies. Previous work (31) showed that labeled sTn exchange was fastest at pCa 4 and that the pattern of exchange became uniform along the thin filament after 2–3 h. Thus, rigor myofibrils were subjected to three rounds of exchange at pCa 4.

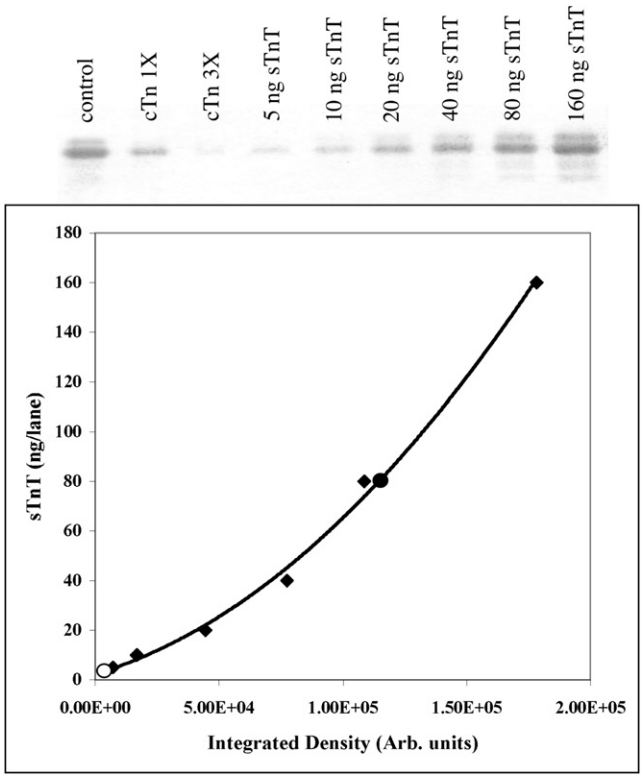

FIGURE 2 Extent of cTn exchange for sTn in skeletal myofibrils. The amount of exchange of cTn for sTn was determined by immunoblotting/densitometric analysis of myofibrils for sTnT. Samples and sTnT standards were subjected to SDS-PAGE and immunoblotting as described in Methods. The upper image shows an immunoblot with the lanes from left to right being control, cTn exchanged one time, cTn exchanged three times, and sTnT standards. The lower graph shows the standard curve with unexchanged myofibrils noted as a solid circle, three times of cTn exchange as an open circle, and sTnT standards as solid diamonds. The exchange procedure resulted in >95% loss of sTnT.

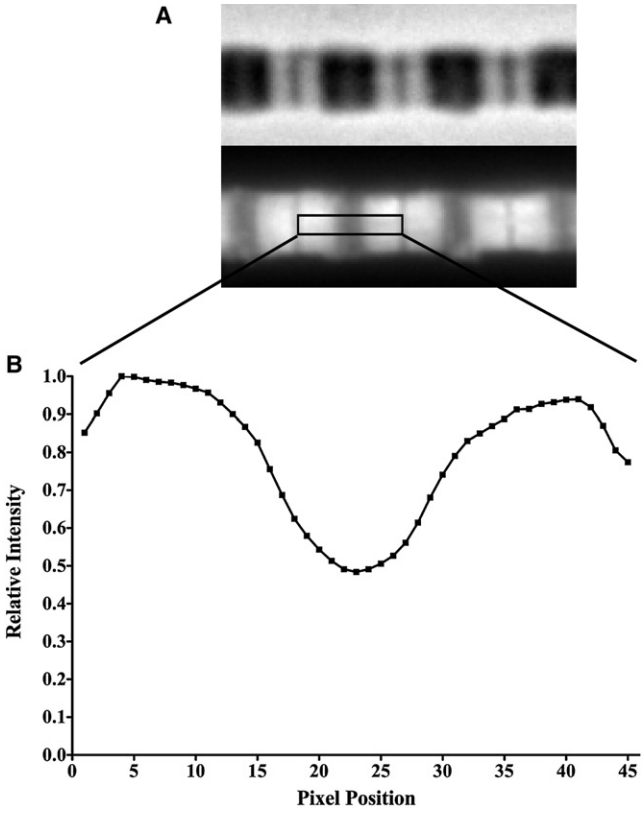

FIGURE 3 Distribution of labeled cTn within a sarcomere. Alexa 488 cTn was exhaustively exchanged into skeletal myofibrils using three exchanges at pCa 4 as in Fig. 2. Myofibrils were imaged and a representative example is shown in *A*. The upper panel is the phase contrast image and the lower is the fluorescence image. The inset represents the region used to determine the column average intensity in *B*.

Fig. 2 shows the extent of exchange of cTn for sTn as determined by quantitative immunoblotting for the loss of sTnT. After the first round of exchange, ~17% of the sTnT remained and after three rounds, only 3.2% ($\pm$2.3%, $n = 3$ immunoblots) remained. The exchange was mostly uniform along the contractile thin filament as shown in Fig. 3, *A* and *B*. The intensity profile within the half sarcomere was more asymmetric than expected with the peak more proximal to the *Z*-line. This same feature was observed in a previous study after extensive exchange (31). In addition, the intensity profile did not reach as low a value in the middle of the A-band as would be expected. This could result from labeled Tn binding to the thick filaments in the nonoverlap region of the A-band. The myofibrils were washed after exchange so it is not likely that this binding was weak. Fig. 4 shows that labeling the cTn did not influence the ATPase activity at pCa 9 or 4 compared with unlabeled cTn. However, cTn resulted in significantly higher pCa 9 and 4 ATPase activities ($p < 0.05$) than sTn myofibrils. The magnitude of the differences in means was greater at pCa 9 (0.021 vs. 0.011 nmol Pi/min/μg) than at pCa 4 (0.41 vs. 0.32 nmol Pi/min/μg). The pCa 9 and 4 ATPase activities are similar to those observed with rabbit psoas myofibrils (39).

Influence of Tn isoform on calcium-sensitive parameters

pCa–ATPase relationship

The calcium-dependent activation of ATPase activity in myofibrils containing cTn were different from those containing sTn (Fig. 5). At pCa 9, the mean values showed similar features as observed in Fig. 4 with cTn myofibrils having higher activity (0.011 vs. 0.008 nmol Pi/min/μg, $p < 0.05$) at pCa 9. The mean values at pCa 4 were not significantly different and cTn myofibril ATPase activity was lower than sTn myofibril ATPase activity (0.34 vs. 0.38 nmol Pi/min/μg, $p > 0.05$). Different myofibril and Tn preparations were used for the experiments in Figs. 4 and 5 but the same exchange protocol was used. The differences in the pCa 9 and 4 ATPase activities could result from subtle differences in the protein preparations. Analysis of ATPase activity as a function of pCa showed that myofibrils containing cTn had a 0.24 pCa unit higher pCa_{50} but a lower Hill

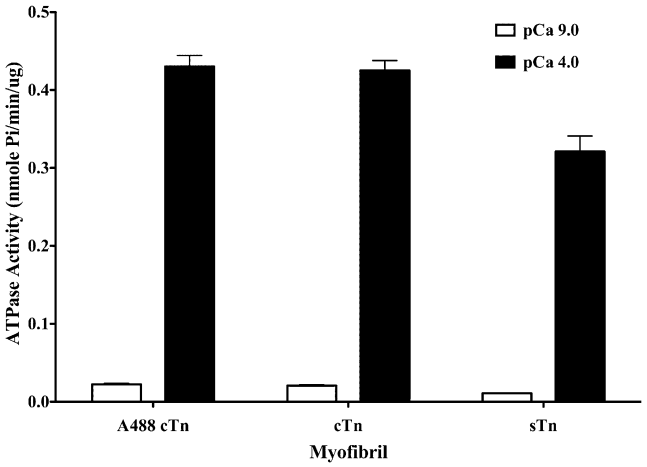

FIGURE 4 ATPase activity at high and low calcium (pCa 9 and 4) for Alexa 488 cTn, cTn, and sTn myofibrils. Fluorescently labeled cTn, unlabeled cTn, or sTn was exchanged into skeletal myofibrils and ATPase activity measured as described in Methods. Data represent the mean + SD ($n = 4$).

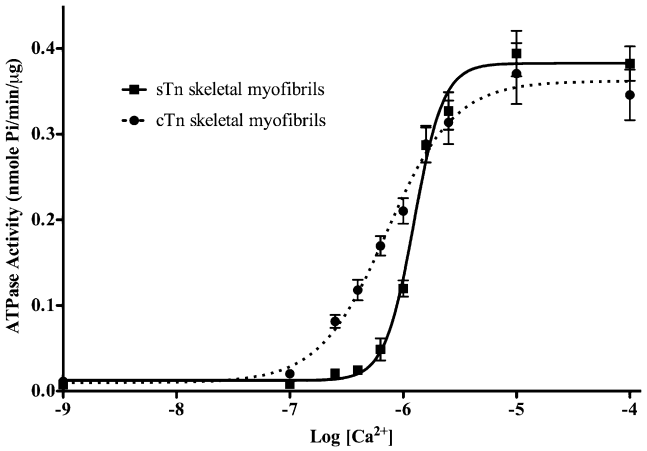

FIGURE 5 Cardiac Tn alters calcium sensitivity of ATPase activity in skeletal myofibrils. The pCa–ATPase activity was measured in sTn and cTn myofibrils as described in Methods, plotted and fitted with a sigmoid logistic equation. The pCa_{50} values were 5.90 (±0.02) and 6.14 (±0.05), whereas the n_H values were 3.36 (±0.44) and 1.46 (±0.24) for sTn (*solid squares*) and cTn (*solid circles*) containing myofibrils, respectively. Data points represent mean ± SD (n = 7–8) and the fitted parameters are the best fit value ± SE of the fitted value.

coefficient (1.46 for cTn compared with 3.36 for sTn). The differences in the calcium-sensitive parameters are similar to those observed in single myofibril force studies (16). They differ from those of Clemmens et al. (41) who observed no difference in the pCa_{50} of actin filament sliding speed when comparing sTn/sTm and cTn/sTm, and a decreased single filament force for cTn/sTm compared with sTn/sTm. The differences in assay conditions and measurements could explain some of the differences between the results.

Tn exchange pattern and rate at pCa 9 and 4

To define the influence of Tn isoform on Tn dissociation rate, the pattern of labeled Tn exchange was determined in rigor myofibrils as a function of time. The pattern for sTn at pCa 9 (Fig. 6 *A upper left panel*) was similar to that observed previously (31) with most of the exchange occurring in the overlap-region early on followed by a gradual increase in the nonoverlap region. By 2048 min, the pattern of exchange was mostly uniform along the full length of the contractile thin filament. The pattern was similar for cTn compared with sTn, with the exception that it was uniform after ~256 min (Fig. 6 *A*, *upper right panel*). At pCa 4, the pattern for sTn was similar to previous studies with exchange occurring faster in the nonoverlap than the overlap region early on and it became equal after ~256 min (Fig. 6 *A*, *lower left panel*). The pattern for cTn was opposite that of sTn. Exchange was slower in the nonoverlap region than in the overlap region, and the extent of exchange became equal after ~64 min (Fig. 6 *A*, *lower right panel*) for cTn. This suggests that calcium had a smaller effect on cTn exchange than sTn exchange in the nonoverlap region.

To estimate the Tn dissociation rate from the different regions of the half sarcomere at pCa 9 and 4, the intensity ratio as a function of time was analyzed as done previously (31). The curves are shown in Fig. 6 *B* and the estimates for the Tn dissociation rates from the different regions are in Table 1. Comparison of the Tn dissociation rates shows that the nonoverlap region rate at pCa 9 was ~10-fold faster (5.1 vs. 0.61 min^{-1}), the nonoverlap region rate at pCa 4 was ~2-fold faster (150 vs. 88 min^{-1}), and the overlap region rate was ~4-fold faster (260 vs. 68 min^{-1}) for cTn compared with sTn. The normalized rates (to the nonoverlap region at pCa 9) show that the relative magnitude of the influence of calcium (nonoverlap region at pCa 4) and rigor cross-bridges (overlap region) was much less for cTn than sTn myofibrils (Table 1). In addition, rigor cross-bridges had a greater effect than calcium on the cTn dissociation rate that is opposite of that observed for sTn.

Tn exchange pattern as a function of pCa

To further understand the influence of calcium on Tn isoform exchange pattern, labeled Tn exchange was done for 8 min as a function of pCa. As noted in Methods, sampling at early time points gives the most information on differences in the Tn dissociation rate between the regions. There was a decrease in the relative signal from the nonoverlap region as pCa increased for both sTn and cTn myofibrils (Fig. 7 *A*); however, the decrease in relative intensity was much more abrupt for sTn (Fig. 7 *A*, *left panel*) than for cTn (Fig. 7 *A*, *right panel*) myofibrils. As observed in previous studies (31), there was faster Tn exchange in the nonoverlap region proximal to the overlap region for sTn at submaximal calcium levels (pCa 5.8 and 6.0). The faster exchange in the proximal region was not apparent for cTn because the intensity was lower in the nonoverlap region even at saturating calcium.

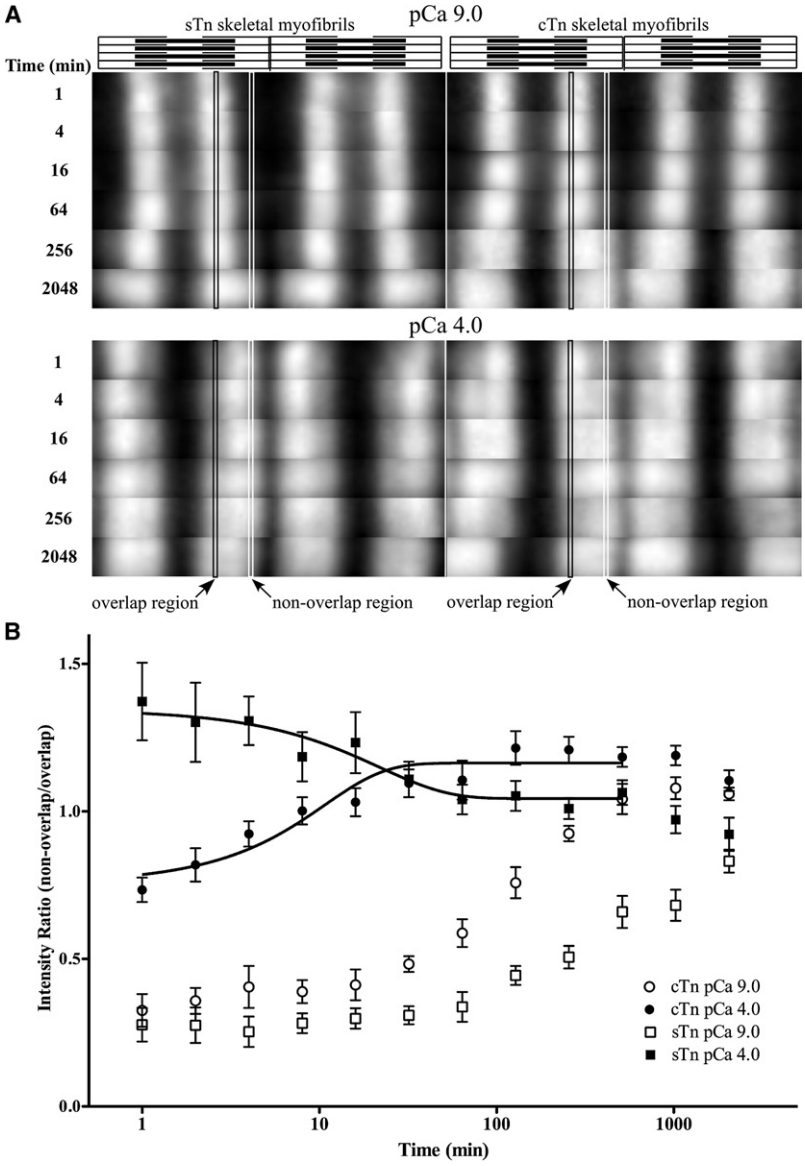

FIGURE 6 The time course of cTn exchange is different than sTn at pCa 9 and 4. Images from labeled sTn exchange into sTn myofibrils (*left panel*) and labeled cTn exchange into cTn myofibrils (*right panel*) at pCa 9 (*upper panel*) and 4 (*lower panel*) are shown in *A*. The intensity was normalized within each image instead of between images to best show the pattern of exchange. Samples were taken at different times and processed as described in Methods. The change in intensity ratio as a function of time is shown in *B*. The ratio was analyzed as described in Methods to estimate the Tn dissociation rate. Data points represent the mean ± SD ($n = 12$–23) with cTn at pCa 9 and 4 as open and solid circles respectively, and sTn at pCa 9 and 4 as open and solid squares respectively. Fitted values are in Table 1.

To graphically show the differences in Tn exchange pattern as a function of pCa, the intensity ratio was plotted as a function of pCa (Fig. 7 *B*). The magnitude of the change in ratio was greater for sTn than cTn myofibrils. However, the change in the intensity ratio as a function of pCa for cTn myofibrils was more sensitive (pCa_{50} of 5.83 and 5.56 for cTn and sTn, respectively), whereas the n_H was lower (1.78 and 2.02 for cTn and sTn respectively) than sTn myofibrils. These trends are similar to those observed for the pCa-ATPase activity relationships but with smaller pCa_{50} and n_H values. This, in part, may be due to the positions used for measurement of the intensity in the different regions, the time point of the exchange, and that ATPase activity is a measure of the fraction of M-state thin filament.

To show the influence of calcium on apparent Tn exchange rate as a function of calcium and location along the thin filament, single sarcomere intensity profiles were obtained from some of the images in Fig. 7 *A* and are shown in Fig. 8. The profiles for sTn are dependent on calcium: the peak is mostly centered in the overlap region at pCa 9, in the nonoverlap region but proximal to the overlap region at pCa 5.8, and near the center of the nonoverlap region at pCa 4. For cTn, the profiles are much different. The peak is near the center of the overlap region independent of calcium but the shoulder on the nonoverlap region is influenced by calcium. The profile for sTn at pCa 5.8 suggests that the Tn sites closest to the strong cross-bridge in the nonoverlap region have a faster dissociation rate. For cTn at pCa 5.8, this feature is not readily apparent in the profile.

Modeling of the intensity profile of a half sarcomere was done to determine if there was nonuniformity in the Tn dissociation rate as a function of distance from the strong-cross-bridge as inferred from the observed profiles. Simple modeling was done as described in the Supporting Material

TABLE 1 Apparent Tn dissociation rates and relative rates

	Tn dissociation rate (10^{-3} min^{-1})*		
Tn	pCa 9 nonoverlap†	pCa 4 nonoverlap‡	pCa 4 overlap‡
sTn	0.61 (± 0.088)	88 (±15)	68 (±11)
cTn	5.1 (±0.97)	150 (±13)	260 (±24)
	Tn dissociation rate relative to pCa 9 nonoverlap region		
sTn	1	144	111
cTn	1	30	50

*Mean +/− standard error of fit.
†Single exponential fit to baseline corrected intensity ratio.
‡From fits shown in Fig. 6.

based on the assumption that the intensity profile is the sum of Gaussian distributions from individual units (Tn exchange sites) along the thin filament. The observed and modeled profiles are shown in Fig. 9 for cTn at pCa 4.0 and 5.8 and sTn at pCa 5.8. Two different models were used to develop the profiles. One was a unitary model where all units within the overlap region had the same magnitude, whereas those in the nonoverlap had a different magnitude but all units within the region had the same magnitude. The other used the same magnitude for all units in the overlap region but graded the magnitude of the units in the nonoverlap region as a function of distance from the overlap region. For both models and all conditions, the model profiles did not match the observed profiles near the middle of the A-band. This could be the result of the labeled Tn binding to the thick filament in the nonoverlap region. In the half I-band region, the models did match the observed profiles, but the quality of the match was pCa and model dependent. At pCa 4, the unitary model profile matched the observed profile for cTn (Fig. 9 *A*). At submaximal calcium, the graded model profiles matched the observed profiles better than the unitary model profiles for both cTn and sTn (Fig. 9, *B* and *C*). Although this simple modeling needs much more development, it strongly suggests that the exchange rate of sTn and cTn at submaximal calcium in the nonoverlap region was dependent on the distance from the rigor cross-bridge.

DISCUSSION

General observations

The extent of cTn exchange was nearly 100% and mostly uniform along the length of the thin filament (Figs. 2 and 3). Comparison of the properties of cTn myofibrils with sTn myofibrils shows four features: 1), cTn does not inhibit the thin filament as much as sTn at pCa 9; 2), cTn can activate myofibrillar ATPase to a similar extent as sTn at pCa 4; 3), cTn is less influenced by calcium than sTn as determined

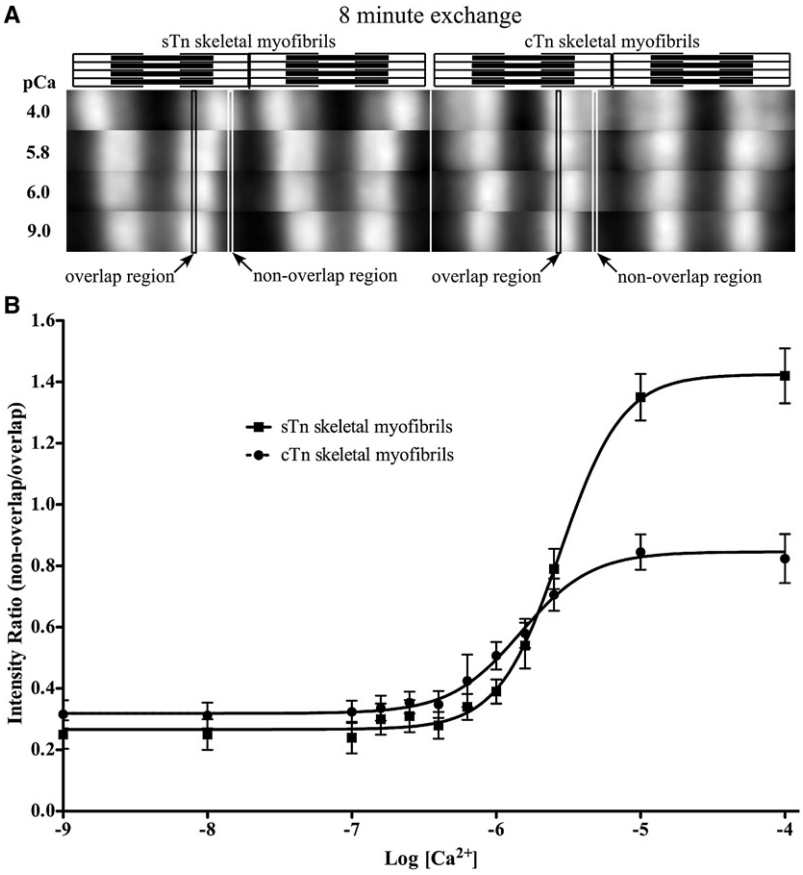

FIGURE 7 The pattern of cTn exchange is different than sTn as a function of calcium. Labeled Tn exchange was done as in Fig. 6 for 8 min and from pCa 9 to 4. Representative images for sTn (*left panel*) and cTn (*right panel*) are shown in *A*. The amount of exchange in the nonoverlap region relative to the overlap region was less for cTn compared with sTn at pCa 4 and showed a more gradual change with an increase in pCa. Also, an enhanced zone of exchange in the nonoverlap region, but proximal to the overlap region, was obvious with sTn at pCa 5.8–6.0, but was not apparent with cTn. The intensity ratio–pCa relationship for sTn (*solid squares*) and cTn (*solid circles*) myofibrils over a range of pCa levels after 8 min of exchange is shown in *B*. The smooth lines represent fits using a sigmoid logistic equation giving a pCa_{50} of 5.56 (±0.01) and 5.83 (±0.02) and an n_H of 2.02 (±0.11) and 1.78 (±0.13) for sTn and cTn, respectively. Data points represent the mean ± SD ($n = 12–22$) and the fitted parameters are the best fit value ± SE of the fitted value.

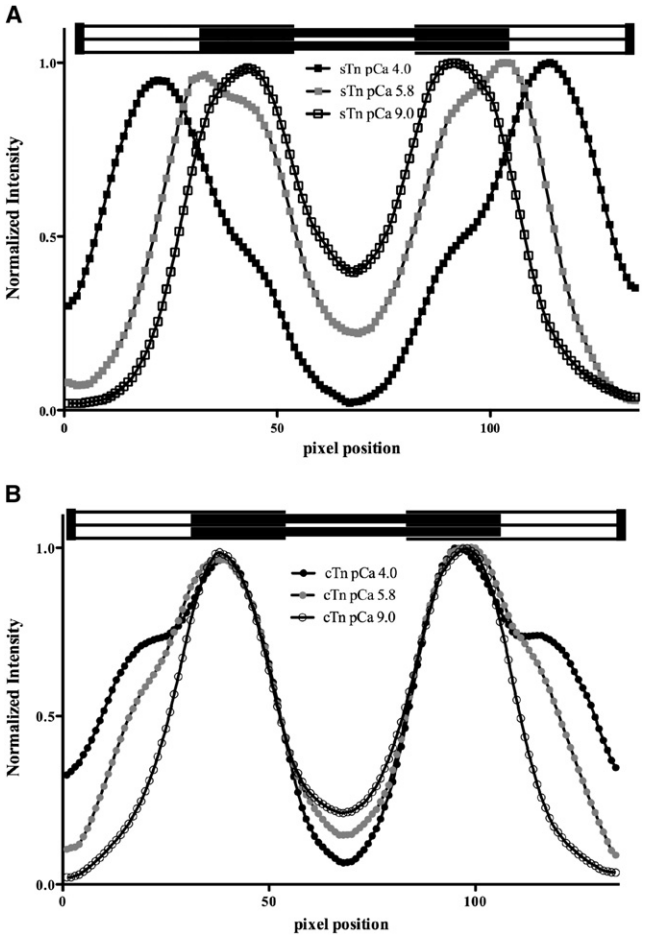

FIGURE 8 Single sarcomere intensity profiles from sTn and cTn myofibrils. Single sarcomere intensity profiles were obtained from the images presented in Fig. 7 as described in Methods. The location of the intensity peak within the half sarcomere varies with calcium for sTn (*A*) but not for cTn (*B*) myofibrils. For sTn, the peak moves from the overlap region toward the nonoverlap region with increasing calcium. For cTn, the peak is in the overlap region independent of calcium and the shoulder of the peak in the nonoverlap region changes with calcium concentration.

from labeled Tn exchange; and 4), cTn has greater calcium sensitivity but lower cooperativity than sTn. In general, these findings are similar to other studies comparing sTn and cTn using either physiological or biochemical methods (16,17,42).

Differential inhibition of the thin filament by cTn and sTn at pCa 9.0

Myofibrils containing cTn had a higher (1.4–1.9-fold) pCa 9 ATPase activity (Figs. 4 and 5) and a 10-fold faster Tn dissociation rate in the nonoverlap region at pCa 9 (Fig. 6, Table 1) than sTn myofibrils. This could result from a small fraction of cTn dissociating from actin-Tm more than sTn during the wash steps after exhaustive exchange, resulting in some unregulated actin-Tm sites. Although this has not been directly ruled out, the cTn exchange patterns suggest that this is not the case. If there were a loss of cTn, one would expect there to be a large difference in the intensity ratio at pCa 9 at early time points when comparing sTn and cTn. This was not observed (Fig. 6). The data for cTn at pCa 9 thus suggest that cTn is less in the off or inactive state than sTn. In terms of the three-state model, this suggests that the B- to C-state equilibrium is shifted more to the C state for cTn than sTn at low calcium. This same feature has been observed in biochemical studies (17,42), and inferred from structural (43) and physiological studies (16).

The molecular mechanisms involved in the cTn thin filament being less inactive at low calcium could be via a weaker TnI–actin-Tm interaction. Biochemical studies showed that cTnI is less effective at inhibiting skeletal actomyosin ATPase activity than sTnI (44,45). TnT could also contribute through its interactions with actin-Tm or TnI and TnC (46). There could also be differences in TnI interaction with actin-Tm because the skeletal myofibril thin filaments also contain nebulin. The issue of cTn not being fully inactivated at low calcium has implications for the molecular mechanisms involved in thin filament activation in general and implications for cardiac physiology and pathophysiology. Simple modeling of the scheme presented below suggests that small changes in the TnI–actin-Tm interaction can impact calcium-sensitivity without there being any changes in TnC properties.

Similar extent of activation by cTn and sTn at pCa 4 even though relative Tn dissociation rates are much different

In terms of the observed pCa 4 ATPase activity, cTn can activate the thin filament to a similar level as sTn (Figs. 4 and 5). This feature was also observed in single myofibril force measurements (16) and with in vitro motility assays (41). In terms of the early exchange pattern, calcium activation of the thin filament gave a higher intensity ratio for sTn than cTn (Figs. 6 and 7). Comparison of the relative (to their respective nonoverlap region pCa 9 exchange rate; Table 1) Tn dissociation rates show that the nonoverlap region at pCa 4 was ~150-fold faster for sTn compared with 30-fold faster for cTn. This suggests that calcium has a much smaller role in changing cTn interaction with the thin filament. This is congruent with the apparent weaker regulatory interactions between cTnC and cTnI compared with sTnC–sTnI (13) and with the small apparent influence of calcium on cTn binding to actin-Tm (47,48). In terms of the three-state model, this suggests that the extent of shifting the thin filament from the B to the C state by calcium is less for cTn than for sTn. This agrees with the observations of Maytum et al. (17) and Bouseff et al. (42). In preliminary experiments (49), labeled Tn exchange was done with sTnC-cTnIT myofibrils. An intensity ratio higher than one at early time points at pCa 4 was observed compared with less than one for cTnC-cTnIT. This suggests that Tn interaction with actin-Tm can be further weakened by a TnC isoform that has greater regulatory conformational changes and a higher affinity for the regulatory domain of

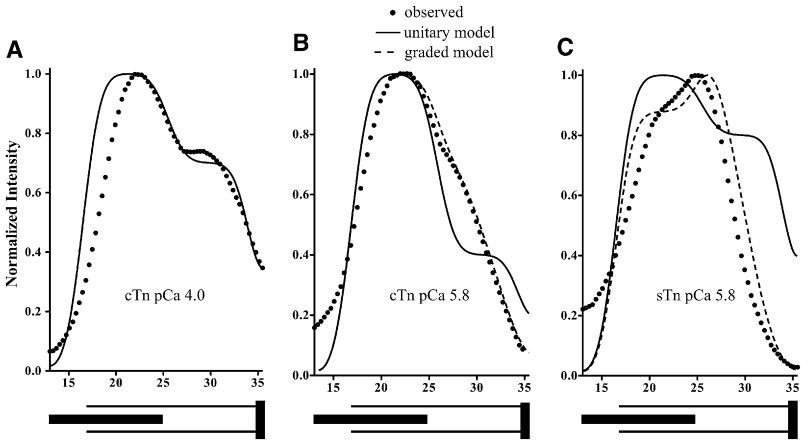

FIGURE 9 Half-sarcomere intensity profile models at pCa 4 and 5.8. Intensity profiles were modeled as the sum of Gaussian profiles for units along the thin filament as described in Supporting Material. The unitary model profile for cTn at pCa 4 matches the observed profile in the nonoverlap region of the half sarcomere (*A*). The graded model profile matches the observed profile better than the unitary model for both cTn (*B*) and sTn (*C*) at pCa 5.8.

TnI. Further studies are needed to characterize the influence of TnC isoforms and/or engineered mutants on thin filament activation as measured by Tn exchange.

If calcium has less of an influence on cTn, then how does cTn give the same extent of activation of ATPase activity at pCa 4 as sTn? One explanation is that cTn is more dependent on the transient strong cross-bridges to activate the thin filament than sTn as inferred from other experiments (50,51). In support of this, the current study shows that the overlap region cTn dissociation rate is faster than the nonoverlap region at pCa 4. Another potential explanation is Tm isoform differences. The current study used skeletal myofibrils and thus α/β Tm, whereas small mammal cardiac muscle mostly has the α-isoform (52). Direct comparison of Tn and Tm isoforms via biochemical experiments showed that thin-filament properties were mostly dependent on Tn isoform instead of Tm isoform (42). Other studies using sTn/sTm and cTn/sTm showed little influence of the Tn isoform on in vitro motility but a large influence of the Tn isoform on single filament force (41). Structural studies on actin-Tm in the absence of Tn suggest that Tm is mostly in the C-state position for sTm and mostly in the B-state position for cTm (23). This difference in the Tm isoforms plus cTn being less off could partially explain how cTn can fully activate actin-sTm with higher calcium sensitivity even though calcium has a lesser influence on cTn. Another possibility is that there are calcium-dependent differences in TnT interactions with actin-Tm. Studies by Dahiya et al. (48), Cassell and Tobacman (53), and Fisher et al. (54) have led to the suggestion that binding of calcium to cTn may decrease TnI binding to actin-Tm but increase TnT binding to actin-Tm. The current studies cannot determine if TnI or TnT mediate the differences in Tn isoform exchange. Further studies are needed to resolve these issues.

Greater calcium sensitivity but lower cooperativity for cTn than sTn

Analysis of the pCa–ATPase profiles and pCa/intensity ratio profiles show that the pCa_{50} is ~0.24–0.27 units more sensitive for cTn than sTn. The direction of the sensitivity difference is the same as that observed by Piroddi et al. (16) but of smaller magnitude. As they pointed out one would not predict higher calcium sensitivity for cTn considering the weaker, calcium induced regulatory interactions between TnC and TnI that is inferred in this study and observed in biochemical studies. In cTn myofibrils, the proportion of inactive or B-state thin filament can be less if the regulatory domain of TnI is not bound to actin-Tm and this may occur without the regulatory domain of TnI binding to TnC. Thus, part of the greater calcium sensitivity could be due to the lower fraction of inactive or B-state actin-Tm sites in the nonoverlap region at pCa 9 for cTn.

The lower cooperativity in the pCa–ATPase data for cTn (1.46 for cTn vs. 3.36 for sTn) is likely mediated by the single calcium-binding site in cTnC compared with sTnC, and this has been shown in several physiological studies (14–16). It could also partially be explained by the system not being as inactive at pCa 9. In general, increases in pCa 9 force or ATPase activity are associated with decreases in cooperativity whether this is mediated by strong cross-bridges (55,56) or changes in apparent TnI–actin-Tm interactions (57). Cooperativity was also observed in the Tn exchange pattern when the intensity ratio as a function of calcium is analyzed (Fig. 7 *B*) and inferred from the modeling of the intensity profiles (Fig. 9). There is an enhanced Tn dissociation rate in the nonoverlap region proximal to the overlap region at submaximal calcium for sTn but this is not as obvious for cTn (Fig. 8). This feature is likely via a long-range effect mediated by Tm, from the strong cross-bridge to Tn (31) and a component of the cooperative mechanism of calcium activation. However, it is difficult to estimate values for the distance of the effect from the images. Toward achieving this goal, the half sarcomere intensity profile was modeled as the result of the sum of Gaussian distributions of light emitted from the Tn sites along the thin filament (Fig. 9). A model that did not incorporate a long-range influence of the strong cross-bridge fit the observed profile at pCa 4 well (Fig. 9 *A*), but it did not fit the observed profiles at submaximal calcium (Fig. 9, *B* and *C*, *unitary model*). These profiles, for both cTn and sTn,

were fit better by a model that incorporated a long-range influence of the strong cross-bridge on Tn that graded with distance from the strong cross-bridge (Fig. 9, *B* and *C*, *graded model*). These observations strongly suggest that there is a long-range (up to 200 nm) influence of the strong cross-bridge on both cTn and sTn as observed in biochemical studies (25,33,34). Much more development of this approach is needed but it will potentially allow for more refined estimates on the influence of the strong cross-bridge on Tn that is likely mediated by Tm.

An alternative Tn dissociation scheme and its relation to thin filament activation

The primary method used in this study to probe Tn interaction with the thin filament was estimation of the rate of Tn dissociation and how this was influenced by calcium and strong cross-bridges. The rate of complete Tn dissociation is likely controlled by TnT dissociation and the dissociation of the C-terminal regulatory domain of TnI that is dictated by the equilibrium of the switching of TnI between actin-Tm and TnC as shown in Scheme 1 (31). The switching of TnI is very rapid (58) and several orders of magnitude faster than TnT dissociation. Kinetic simulations, however, suggest Tn dissociation can be modulated by the switching equilibrium of TnI (A. Sen and D.R. Swartz, manuscript in preparation). The dissociation of TnI from actin-Tm is coupled to its binding to the regulatory domain of TnC as shown in Scheme 1, but this is not a prerequisite for C-state actin-Tm. The observations from the current study suggest that an additional step is needed where TnI first dissociates from actin-Tm and then binds to TnC as shown in Scheme 2. This general scheme is conceptually similar to those presented by Robinson et al. (51) and Maytum et al. (17) but incorporates a step for TnI dissociation from actin-Tm. The first step (K1) is calcium independent, but Tn isoform dependent and likely strong cross-bridge dependent. The second step (K2) is calcium and Tn isoform dependent and may be strong cross-bridge dependent. Tn dissociation from the nonoverlap region at pCa 9 likely follows path K1 to K3′, whereas dissociation at pCa 4 follows path K1 to K3. Comparison of cTn and sTn dissociation rates and ATPase activity at pCa 9 suggest that K1 is larger for cTn than sTn. Comparison of the relative (pCa 4 to pCa 9) Tn dissociation rates in the nonoverlap region suggest that K1*K2 is larger for sTn than cTn. Thus, K2 is smaller for cTn than sTn and this is supported by biochemical data on the calcium dependent interactions between cTnC and cTnI (13) and in reconstituted thin filaments (51). With Scheme 2, modulation of K1 and keeping K2 constant results in a change in the calcium sensitivity of the fraction of C state. In the physiological context, K1 has a finite maximum to allow for inhibition of the system. As it approaches one, the calcium sensitivity becomes K2 (i.e., the pCa_{50} of the thin filament approaches that of Tn alone).

Scheme 1

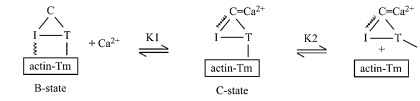

Scheme 2

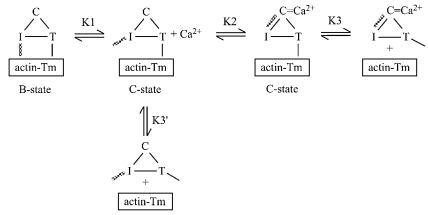

Scheme 2 is supported by this study, biochemical studies with reconstituted thin filaments, and studies on a cTnI mutant associated with hypertrophic cardiomyopathy. Studies on sTn by Rosenfeld and Taylor (59) and cTn by Davis et al. (60) show that calcium binding by Tn differs when Tn is bound to actin-Tm compared with when it is not bound to actin-Tm. The K_d for calcium binding is ~7-fold higher when Tn is bound to actin-Tm compared with when it is not bound to actin-Tm. When rigor S1 and Tn are bound to actin-Tm, the K_d is similar to that of Tn not bound to actin-Tm. Similar observations were made by Robinson et al. (51) on the calcium sensitivity of the distance between cTnI and cTnC. These observations could be partially explained by Scheme 2 where Tn alone has no K1 step, but with actin-Tm-Tn K1 is added and has a small value. However, with rigor S1, K1 becomes larger. For the current work, the proximal rigor cross-bridges increase K1 in a graded fashion giving the enhanced Tn dissociation rate near the overlap region (Figs. 8 and 9). Kobayashi and Solaro (57) showed that the cTnI R145G mutation is associated with an increased basal ATPase activity and calcium sensitivity in reconstituted thin filaments. Mechanical studies with cardiac myofibrils containing this mutation had higher passive tension at low calcium, and this enhanced passive tension was dramatically reduced in the presence of butanedione monoxime suggesting that the thin filament was not completely inhibited (61). These results could be explained by K1 being larger for the mutant than the wild-type, resulting in a greater fraction of C state at low calcium and an increase in calcium sensitivity. There are inter Tn subunit interactions that enhance TnC calcium binding through TnI and TnT (46,62,63) and additional interactions of TnI with actin-Tm that alter calcium sensitivity (57,64) that are not considered in the simple scheme. However, the simple scheme aids in explaining some features of Tn function in thin filament regulation.

In summary, Tn exchange kinetics and ATPase assays were used to investigate the differences between cTn and sTn interactions with skeletal actin-Tm within myofibrils. The data show that cTn is not as inactivated as sTn at low calcium and calcium has a much lesser effect on cTn than

sTn. Although the Tn exchange data show a lesser calcium effect on cTn, it can activate ATPase to the same extent as sTn. Long-range effects between the rigor cross-bridge and Tn are apparent from intensity profile modeling for both sTn and cTn at submaximal calcium. This is likely mediated by a change in the equilibrium between TnI and actin-Tm via a change in the conformation of the actin-Tm binding site of TnI. Further studies using different subunits and mutations of the subunits are needed to fully resolve the differences in the molecular interactions of these Tn isoforms with actin-Tm.

SUPPORTING MATERIAL

One figure is available at http://www.biophysj.org/biophysj/supplemental/S0006-3495(09)00851-0.

The authors thank Dr. K. Byrd and Dr. J. Davis for helpful comments on this work and manuscript.

This work was supported by the American Heart Association, Midwest Affiliate (AHA Fellowship to Z.Y., Grant-in Aid to D.R.S.), and the National Institutes of Health (HL073828 to D.R.S.).

REFERENCES

1. Squire, J. M., and E. P. Morris. 1998. A new look at thin filament regulation in vertebrate skeletal muscle. *FASEB J.* 12:761–771.
2. Farah, C. S., and F. C. Reinach. 1995. The troponin complex and regulation of muscle contraction. *FASEB J.* 9:755–767.
3. Tobacman, L. S. 1996. Thin filament-mediated regulation of cardiac contraction. *Annu. Rev. Physiol.* 58:447–481.
4. Gordon, A. M., E. Homsher, and M. Regnier. 2000. Regulation of contraction in striated muscle. *Physiol. Rev.* 80:853–924.
5. Kobayashi, T., and R. J. Solaro. 2005. Calcium, thin filaments, and the integrative biology of cardiac contractility. *Annu. Rev. Physiol.* 67: 39–67.
6. Dibb, K. M., H. K. Graham, L. A. Venetucci, D. A. Eisner, and A. W. Trafford. 2007. Analysis of cellular calcium fluxes in cardiac muscle to understand calcium homeostasis in the heart. *Cell Calcium.* 42:503–512.
7. Fuchs, F., and S. H. Smith. 2001. Calcium, cross-bridges, and the Frank-Starling relationship. *News Physiol. Sci.* 16:5–10.
8. Konhilas, J. P., T. C. Irving, and P. P. de Tombe. 2002. Frank-Starling law of the heart and the cellular mechanisms of length-dependent activation. *Pflugers Arch.* 445:305–310.
9. Flashman, E., C. Redwood, J. Moolman-Smook, and H. Watkins. 2004. Cardiac myosin binding protein C: its role in physiology and disease. *Circ. Res.* 94:1279–1289.
10. Konhilas, J. P., T. C. Irving, and P. P. de Tombe. 2002. Length-dependent activation in three striated muscle types of the rat. *J. Physiol.* 544:225–236.
11. van Eerd, J. P., and K. Takahshi. 1976. Determination of the complete amino acid sequence of bovine cardiac troponin C. *Biochemistry.* 15:1171–1180.
12. Herzberg, O., and M. N. James. 1988. Refined crystal structure of troponin C from turkey skeletal muscle at 2.0 A resolution. *J. Mol. Biol.* 203:761–779.
13. Li, M. X., L. Spyracopoulos, and B. D. Sykes. 1999. Binding of cardiac troponin-I147–163 induces a structural opening in human cardiac troponin-C. *Biochemistry.* 38:8289–8298.
14. Morris, C. A., L. S. Tobacman, and E. Homsher. 2001. Modulation of contractile activation in skeletal muscle by a calcium-insensitive troponin C mutant. *J. Biol. Chem.* 276:20245–20251.
15. Moss, R. L., M. R. Lauer, G. G. Giulian, and M. L. Greaser. 1986. Altered Ca^{2+} dependence of tension development in skinned skeletal muscle fibers following modification of troponin by partial substitution with cardiac troponin C. *J. Biol. Chem.* 261:6096–6099.
16. Piroddi, N., C. Tesi, M. A. Pellegrino, L. S. Tobacman, E. Homsher, et al. 2003. Contractile effects of the exchange of cardiac troponin for fast skeletal troponin in rabbit psoas single myofibrils. *J. Physiol.* 552:917–931.
17. Maytum, R., B. Westerdorf, K. Jaquet, and M. A. Geeves. 2003. Differential regulation of the actomyosin interaction by skeletal and cardiac troponin isoforms. *J. Biol. Chem.* 278:6696–6701.
18. Fuchs, F., and Y. P. Wang. 1991. Force, length, and Ca(2+)-troponin C affinity in skeletal muscle. *Am. J. Physiol.* 261:C787–C792.
19. Hofmann, P. A., and F. Fuchs. 1987. Effect of length and cross-bridge attachment on Ca^{2+} binding to cardiac troponin C. *Am. J. Physiol.* 253:C90–C96.
20. Wang, Y. P., and F. Fuchs. 1994. Length, force, and Ca(2+)-troponin C affinity in cardiac and slow skeletal muscle. *Am. J. Physiol.* 266:C1077–C1082.
21. Fuchs, F., and D. A. Martyn. 2005. Length-dependent Ca(2+) activation in cardiac muscle: some remaining questions. *J. Muscle Res. Cell Motil.* 26:199–212.
22. McKillop, D. F., and M. A. Geeves. 1993. Regulation of the interaction between actin and myosin subfragment 1: evidence for three states of the thin filament. *Biophys. J.* 65:693–701.
23. Lehman, W., V. Hatch, V. Korman, M. Rosol, L. Thomas, et al. 2000. Tropomyosin and actin isoforms modulate the localization of tropomyosin strands on actin filaments. *J. Mol. Biol.* 302:593–606.
24. Head, J. G., M. D. Ritchie, and M. A. Geeves. 1995. Characterization of the equilibrium between blocked and closed states of muscle thin filaments. *Eur. J. Biochem.* 227:694–699.
25. Maytum, R., S. S. Lehrer, and M. A. Geeves. 1999. Cooperativity and switching within the three-state model of muscle regulation. *Biochemistry.* 38:1102–1110.
26. Smith, D. A., and M. A. Geeves. 2003. Cooperative regulation of myosin-actin interactions by a continuous flexible chain II: actin-tropomyosin-troponin and regulation by calcium. *Biophys. J.* 84:3168–3180.
27. Smith, D. A., R. Maytum, and M. A. Geeves. 2003. Cooperative regulation of myosin-actin interactions by a continuous flexible chain I: actin-tropomyosin systems. *Biophys. J.* 84:3155–3167.
28. Swartz, D. R., M. L. Greaser, and B. B. Marsh. 1990. Regulation of binding of subfragment 1 in isolated rigor myofibrils. *J. Cell Biol.* 111:2989–3001.
29. Swartz, D. R., R. L. Moss, and M. L. Greaser. 1996. Calcium alone does not fully activate the thin filament for S1 binding to rigor myofibrils. *Biophys. J.* 71:1891–1904.
30. Zhang, D., K. W. Yancey, and D. R. Swartz. 2000. Influence of ADP on cross-bridge-dependent activation of myofibrillar thin filaments. *Biophys. J.* 78:3103–3111.
31. Swartz, D. R., Z. Yang, A. Sen, S. B. Tikunova, and J. P. Davis. 2006. Myofibrillar troponin exists in three states and there is signal transduction along skeletal myofibrillar thin filaments. *J. Mol. Biol.* 361: 420–435.
32. Vibert, P., R. Craig, and W. Lehman. 1997. Steric-model for activation of muscle thin filaments. *J. Mol. Biol.* 266:8–14.
33. Greene, L. E., and E. Eisenberg. 1980. Cooperative binding of myosin subfragment-1 to the actin-troponin-tropomyosin complex. *Proc. Natl. Acad. Sci. USA.* 77:2616–2620.
34. Geeves, M. A., and S. S. Lehrer. 1994. Dynamics of the muscle thin filament regulatory switch: the size of the cooperative unit. *Biophys. J.* 67:273–282.
35. Potter, J. D. 1982. Preparation of troponin and its subunits. *Methods Enzymol.* 85:241–263.

36. Fabiato, A. 1988. Computer programs for calculating total from specified free or free from specified total ionic concentrations in aqueous solutions containing multiple metals and ligands. *Methods Enzymol.* 157:378–417.

37. Fritz, J. D., D. R. Swartz, and M. L. Greaser. 1989. Factors affecting polyacrylamide gel electrophoresis and electroblotting of high-molecular-weight myofibrillar proteins. *Anal. Biochem.* 180:205–210.

38. Swartz, D. R. 1999. Exchange of alpha-actinin in isolated rigor myofibrils. *J. Muscle Res. Cell Motil.* 20:457–467.

39. Swartz, D. R., R. L. Moss, and M. L. Greaser. 1997. Characteristics of troponin C binding to the myofibrillar thin filament: extraction of troponin C is not random along the length of the thin filament. *Biophys. J.* 73:293–305.

40. Littlefield, R., and V. M. Fowler. 2002. Measurement of thin filament lengths by distributed deconvolution analysis of fluorescence images. *Biophys. J.* 82:2548–2564.

41. Clemmens, E. W., M. Entezari, D. A. Martyn, and M. Regnier. 2005. Different effects of cardiac versus skeletal muscle regulatory proteins on in vitro measures of actin filament speed and force. *J. Physiol.* 566:737–746.

42. Boussouf, S. E., R. Maytum, K. Jaquet, and M. A. Geeves. 2007. Role of tropomyosin isoforms in the calcium sensitivity of striated muscle thin filaments. *J. Muscle Res. Cell Motil.* 28:49–58.

43. Xu, S., D. Martyn, J. Zaman, and L. C. Yu. 2006. X-ray diffraction studies of the thick filament in permeabilized myocardium from rabbit. *Biophys. J.* 91:3768–3775.

44. Syska, H., S. V. Perry, and I. P. Trayer. 1974. A new method of preparation of troponin I (inhibitory protein) using affinity chromatography. Evidence for three different forms of troponin I in striated muscle. *FEBS Lett.* 40:253–257.

45. Hincke, M. T., W. D. McCubbin, and C. M. Kay. 1977. A circular dichroism and biological activity study on the hybrid species formed from bovine cardiac and rabbit skeletal troponin subunits. *FEBS Lett.* 83:131–136.

46. Gomes, A. V., G. Venkatraman, J. P. Davis, S. B. Tikunova, P. Engel, et al. 2004. Cardiac troponin T isoforms affect the Ca(2+) sensitivity of force development in the presence of slow skeletal troponin I: insights into the role of troponin T isoforms in the fetal heart. *J. Biol. Chem.* 279:49579–49587.

47. Mehegan, J. P., and L. S. Tobacman. 1991. Cooperative interactions between troponin molecules bound to the cardiac thin filament. *J. Biol. Chem.* 266:966–972.

48. Dahiya, R., C. A. Butters, and L. S. Tobacman. 1994. Equilibrium linkage analysis of cardiac thin filament assembly. Implications for the regulation of muscle contraction. *J. Biol. Chem.* 269:29457–29461.

49. Yang, Z. 2005. The exchange of cardiac troponin and its subunits in rabbit psoas rigor myofibrils. *In* Anatomy and Cell Biology. Indiana University, Indianapolis, IN.

50. Bell, M. G., E. B. Lankford, G. E. Gonye, G. C. Ellis-Davies, D. A. Martyn, et al. 2006. Kinetics of cardiac thin-filament activation probed by fluorescence polarization of rhodamine-labeled troponin C in skinned guinea pig trabeculae. *Biophys. J.* 90:531–543.

51. Robinson, J. M., W. J. Dong, J. Xing, and H. C. Cheung. 2004. Switching of troponin I: Ca(2+) and myosin-induced activation of heart muscle. *J. Mol. Biol.* 340:295–305.

52. Wolska, B. M., and D. M. Wieczorek. 2003. The role of tropomyosin in the regulation of myocardial contraction and relaxation. *Pflugers Arch.* 446:1–8.

53. Cassell, M., and L. S. Tobacman. 1996. Opposite effects of myosin subfragment 1 on binding of cardiac troponin and tropomyosin to the thin filament. *J. Biol. Chem.* 271:12867–12872.

54. Fisher, D., G. Wang, and L. S. Tobacman. 1995. NH2-terminal truncation of skeletal muscle troponin T does not alter the Ca^{2+} sensitivity of thin filament assembly. *J. Biol. Chem.* 270:25455–25460.

55. Swartz, D. R., and R. L. Moss. 1992. Influence of a strong-binding myosin analogue on calcium-sensitive mechanical properties of skinned skeletal muscle fibers. *J. Biol. Chem.* 267:20497–20506.

56. Moss, R. L., M. Razumova, and D. P. Fitzsimons. 2004. Myosin cross-bridge activation of cardiac thin filaments: implications for myocardial function in health and disease. *Circ. Res.* 94:1290–1300.

57. Kobayashi, T., and R. J. Solaro. 2006. Increased Ca^{2+} affinity of cardiac thin filaments reconstituted with cardiomyopathy-related mutant cardiac troponin I. *J. Biol. Chem.* 281:13471–13477.

58. Shitaka, Y., C. Kimura, T. Iio, and M. Miki. 2004. Kinetics of the structural transition of muscle thin filaments observed by fluorescence resonance energy transfer. *Biochemistry.* 43:10739–10747.

59. Rosenfeld, S. S., and E. W. Taylor. 1985. Kinetic studies of calcium binding to regulatory complexes from skeletal muscle. *J. Biol. Chem.* 260:252–261.

60. Davis, J. P., C. Norman, T. Kobayashi, R. J. Solaro, D. R. Swartz, et al. 2007. Effects of thin and thick filament proteins on calcium binding and exchange with cardiac troponin C. *Biophys. J.* 92:3195–3206.

61. Kruger, M., S. Zittrich, C. Redwood, N. Blaudeck, J. James, et al. 2005. Effects of the mutation R145G in human cardiac troponin I on the kinetics of the contraction-relaxation cycle in isolated cardiac myofibrils. *J. Physiol.* 564:347–357.

62. Potter, J. D., Z. Sheng, B. S. Pan, and J. Zhao. 1995. A direct regulatory role for troponin T and a dual role for troponin C in the Ca^{2+} regulation of muscle contraction. *J. Biol. Chem.* 270:2557–2562.

63. Davis, J. P., J. A. Rall, C. Alionte, and S. B. Tikunova. 2004. Mutations of hydrophobic residues in the N-terminal domain of troponin C affect calcium binding and exchange with the troponin C-troponin I96–148 complex and muscle force production. *J. Biol. Chem.* 279:17348–17360.

64. Tachampa, K., T. Kobayashi, H. Wang, A. F. Martin, B. J. Biesiadecki, et al. 2008. Increased cross-bridge cycling kinetics after exchange of C-terminal truncated troponin I in skinned rat cardiac muscle. *J. Biol. Chem.* 283:15114–15121.